Figure S1

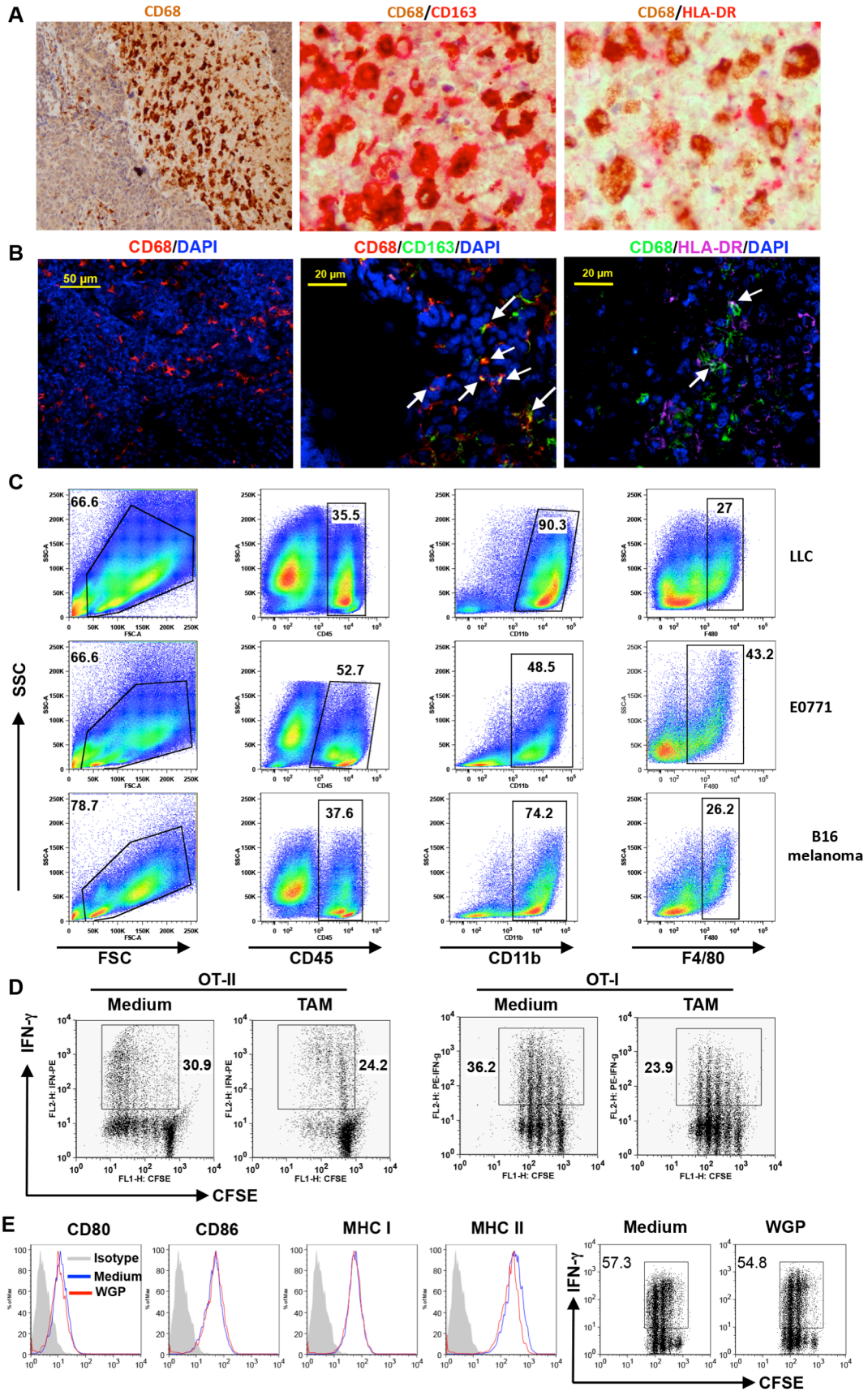
A
CD68
CD68/CD163
CD68/HLA-DR
B
CD68/DAPI
CD68/CD163/DAPI
CD68/HLA-DR/DAPI
50 μm
20 μm
20 μm
C
SSC
FSC
CD45
CD11b
F4/80
LLC
E0771
B16 melanoma
66.6
35.5
90.3
27
66.6
52.7
48.5
43.2
78.7
37.6
74.2
26.2
D
OT-II
OT-I
Medium
TAM
Medium
TAM
IFN-γ
CFSE
30.9
24.2
36.2
23.9
E
CD80
CD86
MHC I
MHC II
Medium
WGP
Isotype
Medium
WGP
IFN-γ
CFSE
57.3
54.8

Figure S1. Human and mouse tumors are abundant with macrophage infiltration. (A) Human breast cancer tissues were stained with CD68 (brown) and CD163 (red) or HLA-DR (red). (B) Cryosection slides of human NSCLC were stained with fluorescent dye labeled mAbs CD68, CD163 or HLA-DR. Diamidino-2-phenylindole (DAPI) staining was used to reveal nuclei. (C) C57Bl/6 mice were implanted with lung cancer LLC, breast cancer EO771, or melanoma B16. When the tumor sizes reached 8-10 mm, mice were sacrificed and single cell suspensions from tumors (n=3) were stained with CD45, CD11b, and F4/80. Representative dot plots are shown. (D) TAM isolated from LLC-bearing mice were stimulated with or without WGP β-glucan for 24 h. Cells were harvested and co-cultured with CFSE-labeled splenocytes from CD4 or CD8 OVA Tg mice in the presence of OVA. Graphs show CFSE dilution versus intracellular IFN-γ on day 3 of culture. Percent of $CD4^+IFN\text{-}\gamma^+$ or $CD8^+IFN\text{-}\gamma^+$ cells is shown. (E) Polarized M1 BMM were stimulated with or without WGP for overnight and cell surface marker expression was determined by flow cytometry. In addition, M1 BMM were co-cultured with purified OT-I CD8 T cells in the presence of OVA for 3 days. Intracellular IFN-γ was stained.

Figure S2

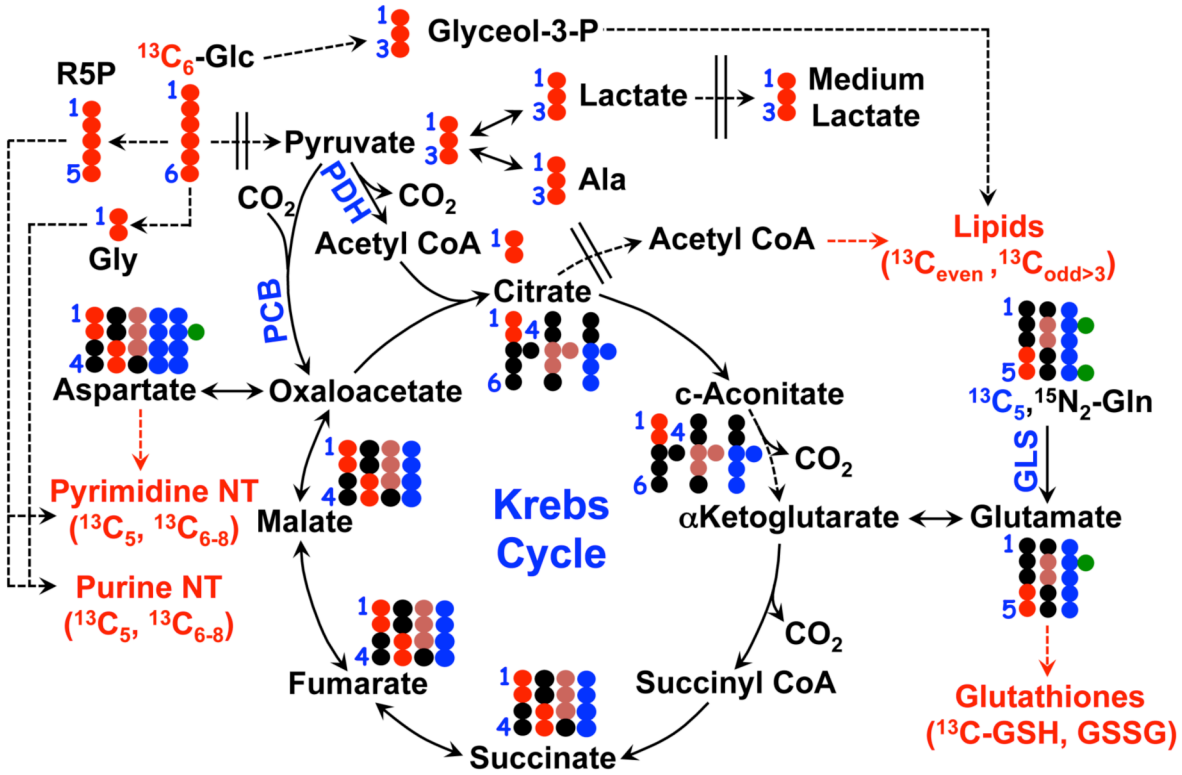

Figure S2. Metabolic pathway tracing from $^{13}C_6$-Glc or $^{13}C_5$,$^{15}N_2$-Gln into lactate, fatty acids, nucleotides (NT), and glutathiones in mouse macrophages. $^{13}C_6$-Glc is converted to $^{13}C_3$-lactate or $^{13}C_3$-glycerol-3-phosphate via glycolysis, which is respectively released into the medium or incorporated into lipids. Glycolytically derived $^{13}C_3$-Pyruvate undergoes pyruvate dehydrogenase (PDH) or pyruvate carboxylase (PCB) reaction for entry into the Krebs cycle, leading to the production of various ^{13}C-labeled Krebs cycle metabolites, which in turn lead to the synthesis of ^{13}C-labeled pyrimidine rings (e.g. $^{13}C_{6-8}$ isotopologues) and fatty acyl chains of lipids (isotopologues with even number or >3 odd number of ^{13}C atom). $^{13}C_6$-Glc is also the precursor to the synthesis of $^{13}C_5$-ribose-5-phosphate (R5P) via the pentose phosphate pathway, which is subsequently incorporated into the purine and pyrimidine NT ($^{13}C_5$ isotopologues). Moreover, the synthesis of $^{13}C_2$-Gly from $^{13}C_6$-Glc via the 3-phosphoglycerate-Ser pathway leads to the production of ^{13}C-labeled purine rings (e.g. $^{13}C_{6-8}$ isotopologues). $^{13}C_5$,$^{15}N_2$-Gln is oxidized by glutaminase (GLS) to Glu before entry into the Krebs cycle to produce $^{13}C_4$-succinate, -fumarate, -malate, -Asp, -citrate, and -cis-aconitate via the 1st turn of the cycle. $^{13}C_4$,$^{15}N_1$-Asp is produced by transamination of $^{13}C_4$-oxaloacetate with $^{13}C_5$,$^{15}N_1$-Glu. Labeled Glu derived from both $^{13}C_6$-Glc and $^{13}C_5$,$^{15}N_2$-Gln is the precursor to the synthesis of ^{13}C labeled glutathione (GSH) and glutathione disulfide (GSSG). Solid single- and double-headed arrows: single step irreversible and reversible reactions; dashed arrows: multi-step reactions or transport across plasma/mitochondrial membrane; ●: ^{12}C; ●,●: ^{13}C from $^{13}C_6$-Glc via PDH or PCB reaction; ●,●: ^{13}C and ^{15}N from $^{13}C_5$,$^{15}N_2$-Gln.

Figure S3

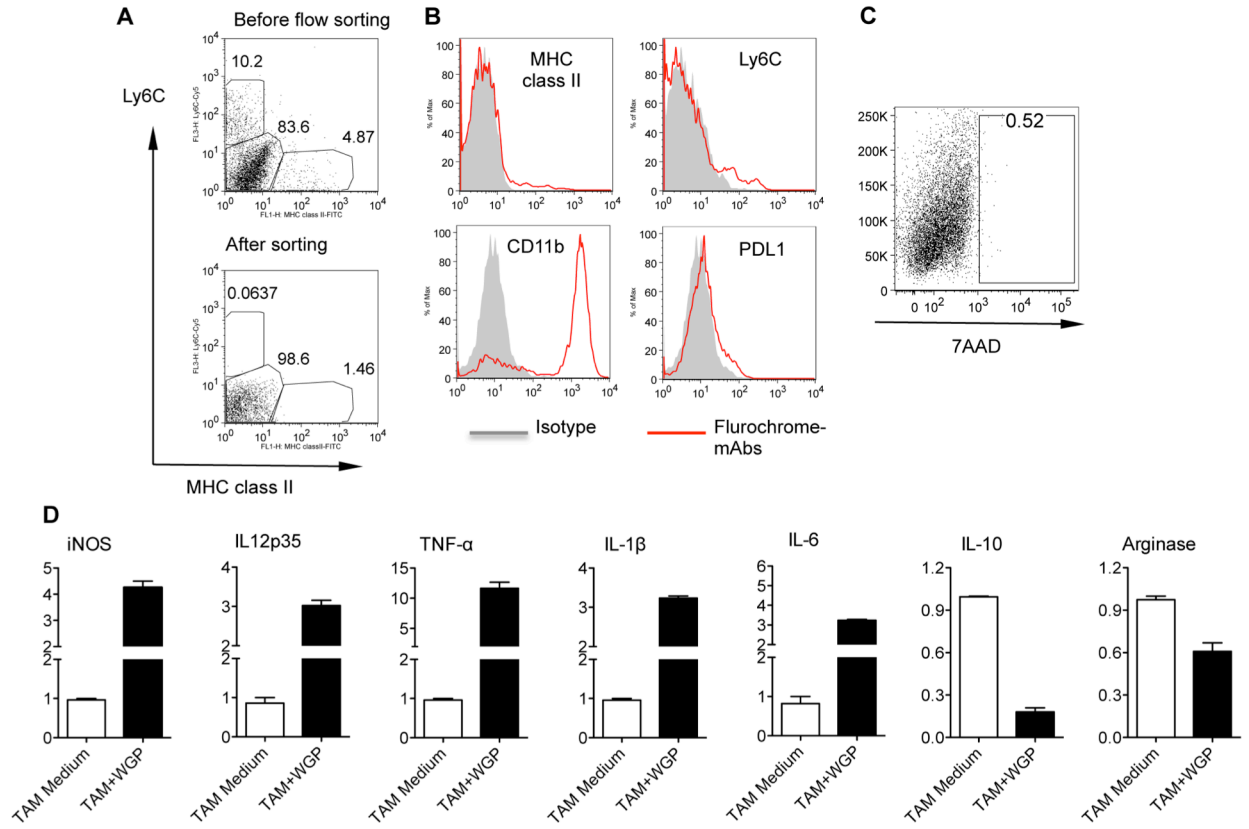

Figure S3. WGP β-glucan treatment converts TAM towards an M1-like phenotype. (A) TAM were first purified using F4/80 microbeads and then further sorted based on Ly6C and MHC class II expression. (B) Sorted TAM are MHC classII^{-}Ly6c^{-}CD11b^{+}PDL1^{lo}. (C) Sorted cells were stained with 7-AAD. (D) Sorted TAM were treated with or without WGP β-glucan for 6 h. The mRNA expression levels of indicated genes were determined by qRT-PCR.

Figure S4

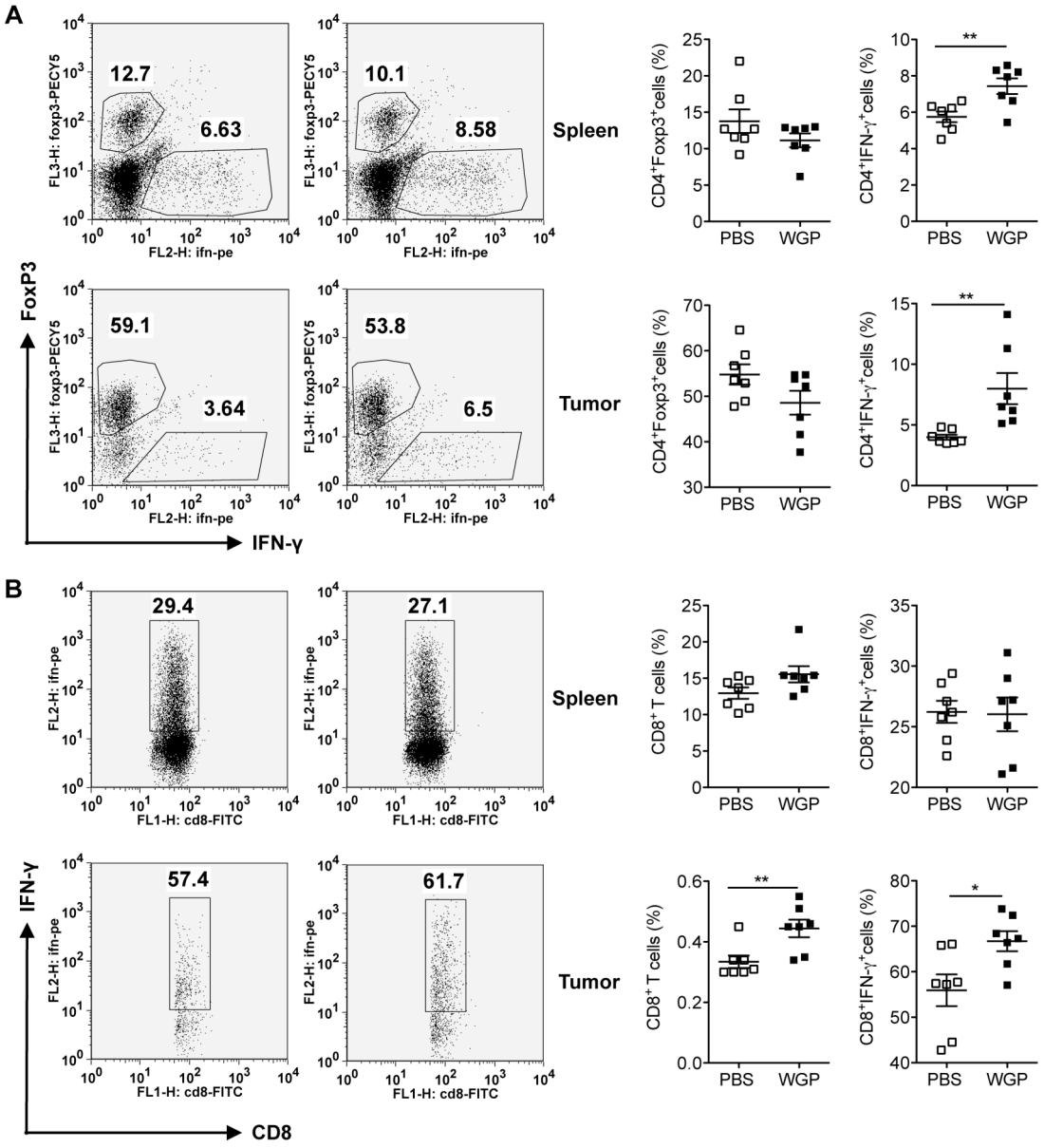

Figure S4. WGP β-glucan in vivo treatment significantly increases IFN-γ-producing CD4 and CD8 T cells. Mice inoculated with murine mammary carcinoma EO771 were treated with WGP β-glucan or PBS for 3 weeks as described in the materials and methods. Single cell suspensions from spleen and tumor were prepared for surface CD4 and CD8 staining as well as intracellular FoxP3 and IFN-γ staining. Cells were gated on $CD4^+$ cells (A) or $CD8^+$ cells (B). Representative dot plots and summarized data are shown. *P<0.05, **P<0.01.